Study on stability and design guidelines for the combined system of scaffolds and shores

Jui-Lin Peng[*1], Chung-Sheng Wang[2a], Shu-Hong Wang[3b] and Siu-Lai Chan[4c]

[1]Department of Civil and Construction Engineering, National Yunlin University of Science & Technology, Yunlin, Taiwan, ROC
[2]Graduate School of Engineering Science and Technology, National Yunlin University of Science and Technology, Taiwan, ROC
[3]School of Resource and Civil Engineering, Northeastern University, Shenyang, China
[4]Department of Civil and Environmental Engineering, The Hong Kong Polytechnic University, Hong Kong, China

Abstract. Since the scaffold is composed of modular members, the total height of multi-story scaffolds does not often meet with the headroom of construction buildings. At this time, other supporting members need to be set up on the top of scaffolds. However, the mechanical behaviors of the combined system of scaffolds and other supporting members have seldom been discussed. This study explores the stability of the combined system of scaffolds and shores. The loading tests conducted in the laboratory show that the critical load of the combined system of two-story scaffolds and wooden shores is about half that of the three-story scaffold system with the same height. In the failure of both the "scaffold system" and the "combined system of scaffolds and shores' after loading, the deformation mainly occurs in the in-plane direction of the scaffold. The outdoor loading test shows that no failure occurs on any members when the combined system fails. Instead, the whole system buckles and then collapses. In addition, the top formwork of the combined system can achieve the effect of lateral support reinforcement with small lateral support forces in the outdoor loading test. This study proposes the preliminary design guidelines for the scaffolding structural design.

Keywords: buckling; critical load; design guidelines; stability; steel scaffold; wooden shore

1. Introduction

On construction sites, door-type steel scaffold is often used in the construction of reinforced concrete structures to serve as temporary supporting structures. Since the total height of multi-story door-type steel scaffold cannot meet with the headroom of the building interior, there often appears to be a gap between the top story of the steel scaffold and the bottom of slabs or beams. In this case, construction workers often use adjustable steel tube shores or wooden shores to fill in the gap. In the paper, this temporary structure installed using scaffolds and shores is simplified and defined as a combined system of scaffolds and shores, as shown in Fig. 1.

In Taiwan, during the construction process, the combined system of scaffolds and wooden shores or adjustable steel tube shores is often used in reinforced concrete structures as falsework. However, until now, engineers seldom directly calculate the load bearing capacity of the entire combined system of scaffolds and shores when conducting the strength design of the combined system. Instead, they calculate and then obtain the load bearing capacities of the steel scaffolds and shores separately, and use the lowest load bearing capacity as the structural design strength. It is debatable whether this structural design method is appropriate or not. Fig. 2 shows the collapse of a combined system of scaffolds and shores on a construction site in Taipei, Taiwan.

In a study on different types of scaffolds, Zhao and Chen (2016) investigated the influence of member imperfection and joint stiffness on the ultimate load of door-type modular steel scaffolding. A novel numerical analysis based on finite element software was adopted. The influence of splice joint stiffness and screw jack stiffness on the ultimate load capacity was investigated. Peng *et al.* (2017) explored the load capacity and failure model of full-scale heavy-duty scaffold systems to elucidate stability behavior. The experimental results revealed that the load capacity and failure model of an independent three-story heavy-duty scaffold were similar to those of the two-story scaffold. Sevim *et al.* (2017) experimentally evaluated the effects of the number of tie bars on the structural behavior of suspended scaffolding systems. Fifteen suspended scaffolding systems were constructed and loaded. Load-displacement curves were obtained and compared to determine the optimal suspended scaffolding system in terms of safety and cost-savings.

In the study of structural scaffolding systems, Kuo *et al.* (2008) explored full-scale loading tests to evaluate the

---

*Corresponding author, Ph.D., Professor
  E-mail: pengjl@yuntech.edu.tw
[a] Ph.D.
  E-mail: johnson.king@yahoo.com.tw
[b] Professor
  E-mail: shwangneu@126.com
[c] Professor
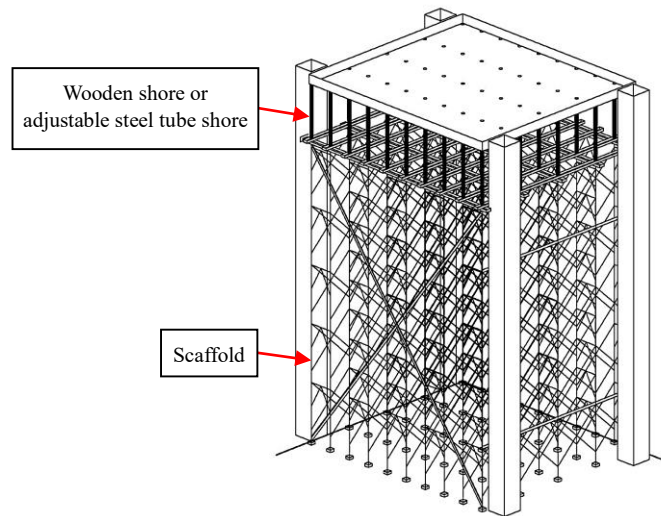 E-mail: siu-lai.chan@polyu.edu.hk

Fig. 1 Schematic diagram of the setup of a combined system of scaffolds and shores

Fig. 2 Collapse of a combined system of scaffolds and shores in Taipei, Taiwan (provided by Professor Jenn-Chuan Chern at National Taiwan University)

performance of an assembly of modular falsework systems with wooden shores under different loading paths. The investigated topics included the relationship between actual load paths and the designed uniform loads, the influence line effect, and the areas of larger axial tube reaction forces. Liu *et al*. (2010a, b) presented the stability of structural steel tubes and coupler scaffolds without and with X-bracings. Twelve full-scale specimens without X-bracings and two full-scale specimens with X-bracings were constructed and tested in the lab. Advanced nonlinear finite element analysis was conducted to compare with experimental results. Liu *et al*. (2016) presented the stability of steel tube-coupler scaffolds with upper horizontal tubes to transfer construction loads. Four specimens were constructed and tested. A finite element analysis using ANSYS was conducted on the specimen models.

Chandrangsu and Rasmussen (2011) proposed methods for modelling spigot joints, semi-rigid connections, and base plate eccentricities. Three-dimensional advanced analysis models were developed to capture the behavior of support scaffold systems. Peng *et al*. (2015) explored the load-carrying capacities of single-row steel scaffolding systems with various setups. When multi-bay setups are used, the load-carrying capacities of the two-story door-type steel scaffolds increase with the number of bays.

Regarding research on the reliability of scaffolds, Zhang *et al*. (2010) investigated the effect of uncertainties on the ultimate strength of multi-story scaffolds through a rational statistical framework and a second-order inelastic finite element analysis. The basic random variables and the model uncertainty were propagated through Monte Carlo simulation to obtain the statistics of system strength. Zhang

et al. (2012) presented a reliability analysis for scaffolds and a second-order inelastic analysis model. The paper investigated the failure mode, the effects of different random variables on the variability of structural strength and the reliability of the scaffolds.

As for the research on the joints, Prabhakaran *et al.* (2011) presented an algorithm to completely model the behavior of scaffold connections. Different approximations to the moment-rotation curves were developed and applied to simple frames. Pieńko and Błazik-Borowa (2013) explored the numerical analysis of a node in modular scaffolds. The load-carrying capacity of the node was based on the numerical analysis considering the nonlinear material and the joint interactions. Jia *et al.* (2016) presented an experimental study on slipping and rotational stiffness in the right-angle coupler connection. They considered bolt tightening torques, new and old conditions of components, different coupler combinations, and loading patterns.

In the study of façade scaffolds, Yue *et al.* (2005) explored the shape coefficient of wind pressure on scaffolds based on wind tunnel tests. By using random vibration theory, formulae were obtained for predicting the wind vibration coefficients of the scaffolds at the two stages of climbing up and down. Ilcik *et al.* (2016) developed a new scaffold anchor system. A finite element model of the scaffold anchor system was updated using experimental data. These investigators updated the finite element model to calculate accurate loading forces on scaffold anchor systems. Błazik-Borowa and Gontarz (2016) presented static non-linear calculations in reference to typical façade scaffolds and analyzed the influence of the dimension and localization of imperfections. They found that the geometrical imperfections caused the increase of internal forces, and the highest increase occurred in the lowest elements. Gohnert *et al.* (2016) presented an experimental investigation on the load capacity of scaffolds. They found that missing bracing could not only lead to a significant reduction of load capacity, but also sudden collapse due to large sway and little sway restraints. Cimellaro and Domaneschi (2017) analyzed the main flaws and imperfections that could cause the collapse of the scaffolds. They proposed an empirical formula to identify the critical scaffold load based on different numbers of stories and boundary conditions.

As shown by the above prior studies on scaffolds, most researchers so far have been focused on pure steel scaffolds. There is limited research on the mechanical behavior of the combined system of scaffold together with other top shores. However, the fact that the headroom of the building interior is not a multiple of the height of a single scaffold is a current problem. This study aims to explore the stability behavior of the combined scaffold and top shore system.

Loading tests and numerical analyses are used to conduct the study. In addition to carrying out the loading tests of the scaffold system and the combined system of scaffolds and shores in the laboratory, this study also conducts an outdoor full-scale test of the combined system of scaffolds and shores. In order to confirm the stiffnesses of various joints in these two systems, this study used the second-order elastic analysis with semi-rigid joints to verify the results of these tests. Based on the results of this study, the preliminary structural design guidelines for the combined system of scaffolds and shores are proposed to serve as a reference for the future scaffold design.

2. Cross-sectional dimensions and material properties

The setups of the two- and three- story scaffolds are shown in Fig. 3. The mean values of the measured cross-sectional dimensions are as follows. The main tube (cross section A-A) has an outer diameter of 42.25 mm and a thickness of 1.92 mm. The horizontal bar (cross section B-B) has an outer diameter of 42.34 mm and a thickness of t = 1.72 mm. The diagonal brace (cross section C-C) has an outer diameter of 26.67 mm and a thickness of 1.33 mm. The cross brace (cross section D-D) has an outer diameter of 21.19 mm and a thickness of 1.46 mm.

The mean values of the steel tube properties of the scaffold system obtained from material tests are as follows: the elastic modulus $E = 203$ GPa, the yield stress $F_y = 35.6$ kN/cm^2, and the ultimate stress $F_u = 499.9$ kN/cm^2.

In the combined system of scaffolds and shores, the wooden shores are set up on top of the scaffolds. The wooden shores are made of Kapur, which is a popular material for wooden shores on construction sites in Taiwan. The mean value of the measured cross-sectional area is 5.630 cm × 5.882 cm. The mean values of Young's modulus and yield stress of the wooden shore as obtained from material tests are 1.247×10^6 N/cm^2 and 4,579 N/cm^2, respectively.

3. Numerical analysis

In this study, the numerical analysis was conducted using a second-order elastic analysis with semi-rigid joints. NIDA (2018), an innovative second-order analysis and design software program developed by Chan *et al.* (1994, 1995), was used for the analysis. In the analysis, the initial imperfection of the scaffolding structure was considered and conditions such as the *P-Δ* effect and *P-δ* effect were additionally included to fully present the real conditions of the scaffolding structure after being loaded.

Over the past years, several studies have been made on the second-order analysis or the direct analysis method. Chan *et al.* (2019) investigated two types of steel frames with asymmetrical beam-to-column joints by direct analysis based on the plasticity. Liu *et al.* (2018) proposed a curved quartic-function beam-column element with the fourth-order polynomial shape function for the design of steel structures by the direct analysis method. Nguyen *et al.* (2016) explored the coupling effects of nonlinearity, geometric imperfections, and residual stress of planar steel frames abased on the second-order distributed plasticity analysis with semi-rigid beam-to-column connections. For other studies related to the second-order analysis, Thai et al. (2017) developed a computer program to predict the second-order inelastic behavior of space steel frames.
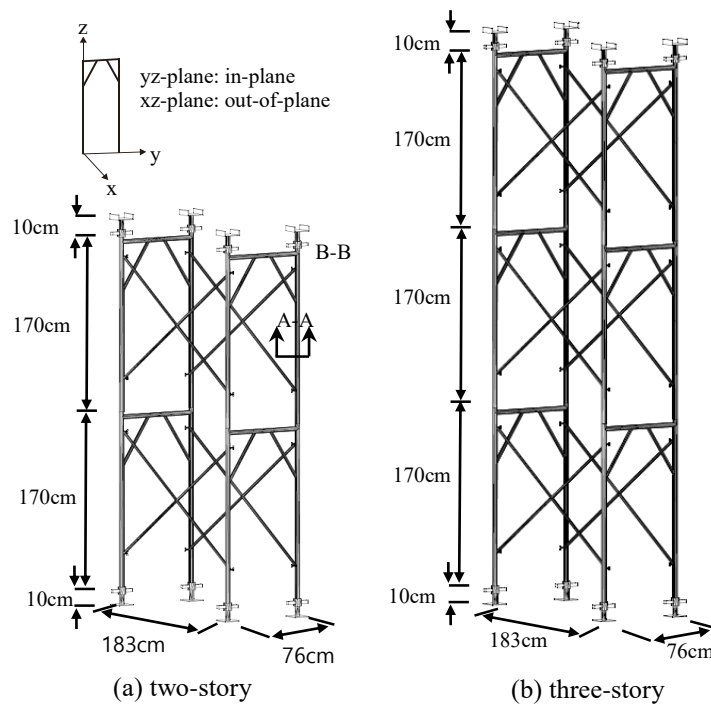
Fig. 3 Test setups of one-set two-story and three-story scaffold systems

The second-order analysis with semi-rigid joints is suitable for structures with a large slenderness ratio, particularly scaffolding structures. In the numerical analysis, in order to simulate the initial imperfection of the overall scaffolding structure, the notional lateral forces (NLFs) were applied in the directions of the two mutually perpendicular axes in the middle of the scaffolding structure.

4. Test planning

The tests conducted in this study are divided into two parts: (1) experimental loading tests on the scaffold system and the combined system of scaffolds and shores, and (2) an outdoor loading test of the full-scale combined system of scaffolds and shores.

4.1 Testing the scaffolds in the laboratory

4.1.1 Tests on one-set steel scaffolds

In this study, loading tests on the two-story and three-story scaffold systems were conducted in the testing laboratory. Dimensions of the two-story and three-story scaffold systems are shown in Figs. 3(a) and 3(b). Two types of boundary conditions were employed in the tests. The first is a case without a bottom screw jack and without a U-shaped top screw jack, and second is a case with a bottom screw jack and with a U-shaped top screw jack.

For the case without a bottom screw jack and without a U-shaped top screw jack, the steel plates on the bottom screw jack and the U-shaped top screw jack were cut off to remove their bending resistance capability. In the analysis,

the upper and lower boundary conditions of the scaffold system can be considered as hinged ends.

4.1.2 Tests on the combined system of scaffolds and shores

In the test setup of a one-bay combined system of two-story scaffold and one-story wooden shores as shown in Fig. 4(a), the 1.7 m long wooden shores were set up on the horizontal wooden stringers over the U-shaped top screw jack. Apart from tests on the one-bay combined system of scaffolds and shores, tests on the two-bay combined system were also conducted as shown in Fig. 4(b). By comparing test results of one-bay and two-bay scaffold systems, this study explores the effect of the number of bays on the load bearing capacity of the combined system of scaffolds and shores.

4.2 Outdoor full-scale test of the combined system of scaffolds and shores

4.2.1 Structural setup

To simulate the setup of scaffolds in reinforced concrete walls and columns on construction sites, a 6 m × 6 m × 6 m steel frame was built in which the combined system of scaffolds and shores was set up in the frame. The base soil was compacted before the test and precast concrete slabs were laid on the base to avoid the base soil from unevenly settling during testing.

In the combined system of scaffolds and shores, the scaffold was setup as a two-story, two-row, and two-bay system. The distance between rows was 76 cm, exactly the width of a door-type steel scaffold. Additionally, 170 cm
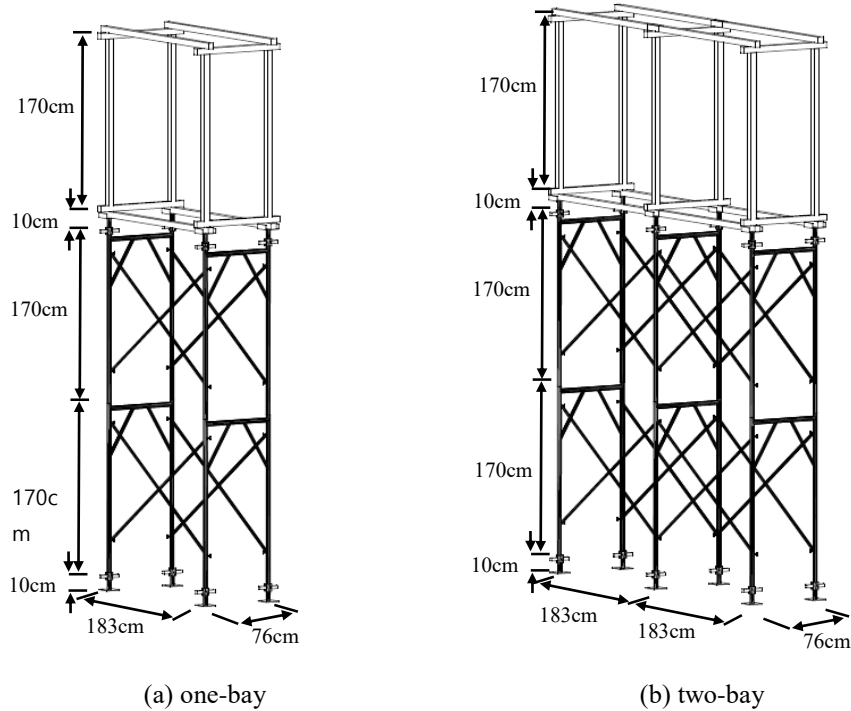
(a) one-bay (b) two-bay

Fig. 4 Test setups of one-bay and two-bay combined systems of scaffolds and shores
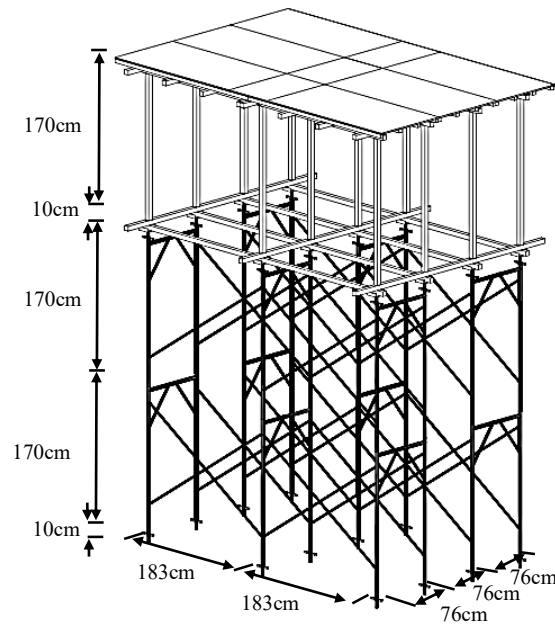

Fig. 5 Setup of outdoor loading test of the full-scale combined system of scaffolds and shores

long wooden shores were set up on the top of the scaffold. The configuration of the combined system is shown in Fig. 5.

For the test, all steel plates on the bottom screw jacks were cut off, so the bottom screw jack can be considered as a hinged end in the later numerical analysis. To simulate the slab on construction sites, the wooden formwork was used to make a 2.7 m x 4.2 m slab and four 6 m long galvanized iron pipes (GIPs) were connected to the slab. Both ends of the GIPs were equipped with a roller, which was set in the

Fig. 6 Lateral bracing at the top formwork in the outdoor loading test of the combined system of scaffolds and shores

Fig. 7 Setup of the combined system of scaffolds and shores in the outdoor loading test on site

rail on the frame. When the slab bears a vertical load, the overall slab can only move downward in the vertical direction due to the constraint of the GIPs. The setup of the lateral bracing for the slab is shown in Fig. 6. This setup simulates the lateral restraint of the concrete columns and walls of the building being constructed. The restraint can only make the slab move vertically downward. The overall configuration of the full-scale combined system of scaffolds and shores in the outdoor test is shown in Fig. 7.

Theodolites were used to measure displacements during the outdoor test. Fig. 8 shows the observation positions of theodolites. A_H refers to the lateral displacement between the wooden shores and scaffolds at the southern side joints. B_H and B_V refer to the lateral and vertical displacements at the top-end of the wooden shores on the southern side. C_H

refers to the lateral displacement at the eastern side joints between the wooden shores and scaffold. D_H and D_V refer to the lateral and vertical displacements at the top-end of the wooden shores on the eastern side.

For the vertical scaffold steel tubes, there are three rows (A, B, C) in the Y direction and four vertical steel tubes in each row in the X direction. Therefore, there are 12 vertical steel tubes in total. Prior to testing, four strain gauges were attached on each of the 12 vertical steel tubes to measure the change in axial force for each vertical steel tube as shown in Fig. 9. In addition, four strain gauges were attached to each of the four horizontal GIPs (H1~H4) to measure the lateral force of each GIP.
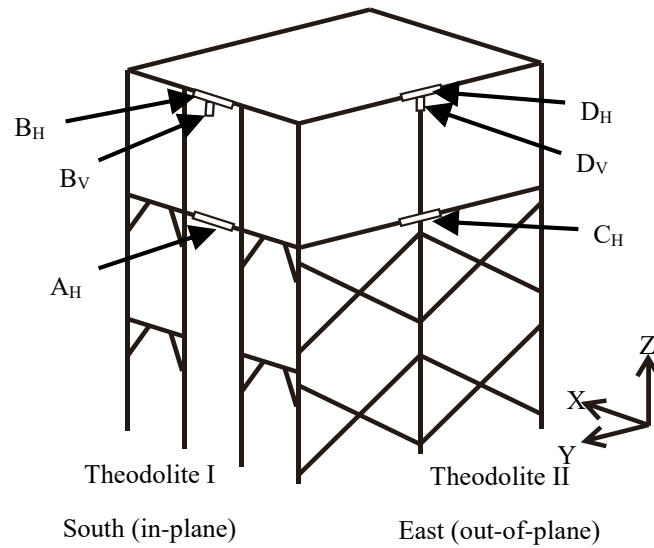
Fig. 8 Positions of the theodolites and measuring points of the combined system of scaffolds and shores in the outdoor loading test
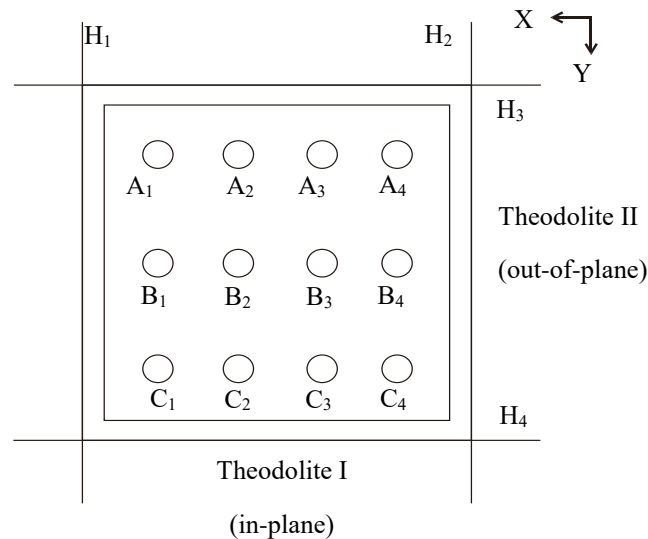

Fig. 9 Positions of the strain gauges for the combined system of scaffolds and shores in the outdoor loading test

4.2.2 Load setup

In the outdoor test, sandbags were used to simulate fresh concrete placed on the slab. Prior to testing, many sandbags weighing around 500 kg each were placed in the sandbag stowage area. During testing, a crane scale was attached to the hook of the crane. When a sandbag was lifted, its correct weight was read. The sandbag was then placed at a predetermined position and sequence on the slab. In principle, the sandbags are evenly placed on the slab in a bilaterally and diagonally symmetrical manner. The predetermined placing sequence for each story is shown in Fig. 10.

5. Test & analysis results and discussions

5.1 Indoor one-set steel scaffolds

5.1.1 Tests on one-set steel scaffolds
A. Bottom screw jack and U-shaped top screw jack without plates

● **Testing**
Before the tests, the steel plates of the bottom screw jack and the upper U-shaped top screw jack, which were used to adjust the height of the scaffold, were cut off. The test results can be treated as the lower limit of the load bearing capacity of the scaffold structure. As shown in Table 1, the
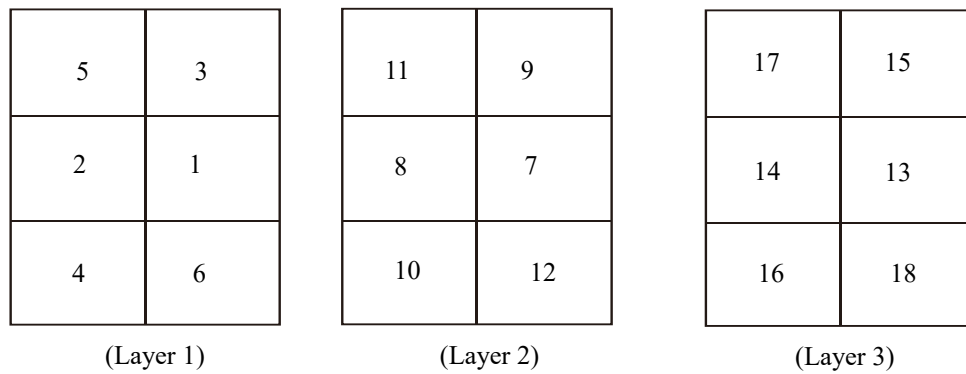
5	3
2	1
4	6

(Layer 1)

11	9
8	7
10	12

(Layer 2)

17	15
14	13
16	18

(Layer 3)

Fig. 10 Schematic diagram of the sequence of sandbags placed on the slab.

(A) Two-story

(B) Three-story

Fig. 11 Failure shapes of two-story and three-story scaffold systems without the plates of bottom screw jack and U-shaped top screw jack in tests

mean load bearing capacities of the two-story and three-story scaffold systems are 107.62 kN and 97.87 kN respectively. The three-story scaffold system has 0.91(=97.87/107.62) of the mean load bearing capacity of the two-story scaffold system. After loading, the deformation of both the two-story and three-story scaffold systems mainly occurred in the in-plane direction of the scaffold. The failure shape of one-set, three-story scaffold system without the plates of the bottom screw jack and U-shaped top screw jack after loading is shown in Fig. 11.

● **Analysis**

A second-order elastic analysis with semi-rigid joints was conducted for both the two-story and three-story scaffold systems without the plates of the bottom screw jack and U-shaped top screw jack. The analysis results are shown in Table 1. In the analysis, the upper and lower boundary conditions of the scaffold system were considered as hinged ends. The cross brace can be considered as a two-force member and its ends can be assumed as hinged ends. The joint stiffness of the vertical steel tubes in the scaffold system was estimated by trial and error. The bending moment stiffness of the steel tube joints was found to be

Table 1 Comparison of test and analysis results for loading tests on the scaffold system and the combined system in the testing laboratory

Type	Setup	Graph	No.	Test kN (I)				Analysis kN (II)	(I)/(II)	Define different joint stiffnesses
				Group A	Group B	Group C	Average			
2-story 1-bay structural system	Without bottom screw jack/ Without U-shaped top screw jack		2DSBNUJN	102.91	112.23	---	107.62	112.23	0.96	1. Tube joint stiffness = 2943 kN-cm/rad
										2. Base stiffness = 98 kN-cm/rad
	With bottom screw jack/ With U-shaped top screw jack		2DSBUJ	115.76	106.63	---	111.25	115.27	0.97	3. End condition of cross braces = pinned end
3-story 1-bay structural system	Without bottom screw jack/ Without U-shaped top screw jack		3DSBNUJN	94.57	103.79	95.26	97.87	97.71	1.00	
	With bottom screw jack/ With U-shaped top screw jack		3DSBUJ	96.73	101.44	---	99.08	107.62	0.92	
Combined system of scaffolds and shores	1-bay 2-story scaffolds with wooden shores		WS2D$_s$	54.15	43.46[#]	48.85	48.82	52.22	0.93	1. Tube joint stiffness = 2943 kN-cm/rad
										2.Hinged base
	2-bay 2-story scaffolds with wooden shores		WS2D$_s$2B	88.00	79.66	---	83.88	78.68	1.07	3. End condition of cross braces = pinned end
										4. Joint stiffness between scaffold and wooden shore = 981 kN-cm/rad

Note: "---" refers to no test value.

2943 kN-cm/rad (300 tonne-cm/rad). Based on the joint stiffness, the analysis values for the two-story and three-story scaffold systems were obtained as 112.23 kN and 97.71 kN respectively. These are very close to their test values (107.62 kN and 97.87 kN). The comparison of the test and analysis results for the scaffold system is shown in Table 1.

Fig. 12 shows the *P-Δ* curves from the second-order analysis of a two-story scaffold system without the plates of the bottom screw jack and U-shaped top screw jack. As shown in Fig. 12, various NLFs (e.g., NLF = 0.10%, 0.05%, and 0.01%) tend to approach the same value based on elastic materials of scaffolds.

In the second-order analysis by NIDA, the first eigen-shape of the scaffold structure can also be used to simulate the initial imperfection. As shown by the *P-Δ* curves in Fig. 12, the initial imperfections of H/200 (=0.005H) and H/1000 (=0.001H) of the first eigen-shape are larger than NLF = 0.1%. In this study, because the critical load can be easily interpreted in *P-Δ* curves, in principle, NLF = 0.01% is used as the initial imperfection in the numerical analysis.

B. Bottom screw jack and U-shaped top screw jack with plates

The tests in this section were conducted on the scaffold system with the bottom screw jack and U-shaped top screw jack. The test results can be treated as the upper limit of the load bearing capacity of the scaffold structure. As shown in Table 1, the mean load bearing capacities of the two- and three-story scaffold systems are 111.25 kN and 99.08 kN, respectively. After loading, the deformation of both the two-story and three-story scaffold systems mainly occurred in the in-plane direction of the scaffold.

In the case of the two-story scaffold system, the load bearing capacity of the system with the bottom screw jack and U-shaped top screw jack is 1.03 times (=111.25/107.62) that of the system without the plates of the bottom screw jack and U-shaped top screw jack. Similarly, the three-story scaffold system with the bottom screw jack and U-shaped top screw jack is 1.01 times (=99.08/97.87) that of the system without the plates of the bottom screw jack and U-shaped top screw jack. The bending stiffness of the bottom screw jack and the U-shaped top screw jack used in this study insignificantly enhances the load bearing capacity of the scaffold systems.
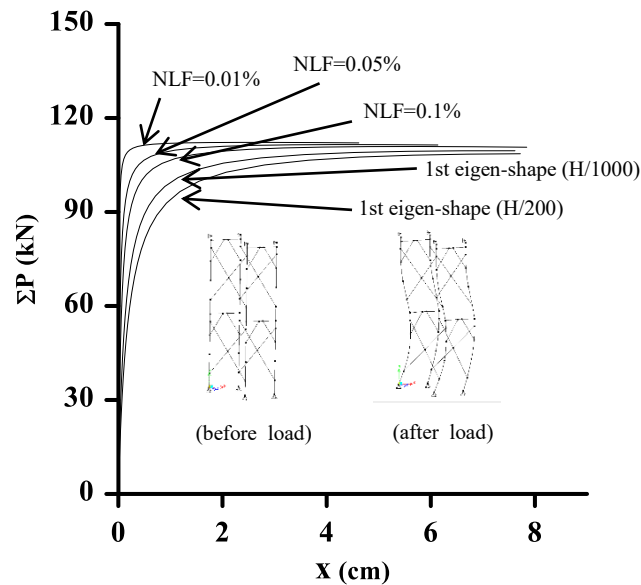
Fig. 12 *P-Δ* curves from the numerical analysis of two-story scaffold system without the plates of bottom screw jack and U-shaped top screw jack

The bending stiffness of the joints at the bottom screw jack and U-shaped top screw jack of the scaffold system can be obtained by comparing the analysis results with the test results by trial and error. They are 98 kN-cm/rad.

5.1.2 Tests on combined system of scaffolds and shores

A. One-bay system

The mean load bearing capacity of the combined system of scaffolds and shores was 48.82 kN, as shown in Table 1. The deformation mainly occurred at the joints between the scaffold and wooden shores and in the in-plane direction of the scaffold. The failure shape is shown in Fig. 13(a). Comparing the test results of the above combined system to those of a three-story scaffold system with the same height (510 cm), the load bearing capacity of the combined system is 0.5 times (= 48.82/97.87) that of the three-story scaffold system. It is obvious that, with the same height, the load bearing capacity of the combined system is far lower than that of the scaffold system without shores.

As shown in Table 1, in the numerical analysis, the load bearing capacity of the one-bay combined system is 52.22 kN. Fig. 14 shows the *P-Δ* curve of the one-bay combined system of scaffolds and shores. In the numerical analysis, the bending stiffness at the joints between the wooden shores and scaffold was obtained as 981 kN-cm/rad by trial and error. The deformation mainly occurred at the joints between the scaffold and the wooden shores and in the in-plane direction of the scaffold.

B. Two-bay system

As shown in Table 1, the mean load bearing capacity of the two-bay, two-story combined system of scaffolds and shores was 83.88 kN. The deformation mainly occurred at the joints between the scaffold and wooden shores and in the in-plane direction of the scaffold. Fig. 13(b) shows the

failure shape of the two-bay, two-story combined system obtained after testing. As shown in Table 1, the load bearing capacity of the combined system increases alongside with increase of bay numbers; however, it does not do so in integral multiples. The raise in this study is 1.7 (=83.88/48.82) times.

Settings of the two-bay combined system of scaffolds and shores are the same as those of the one-bay system in the analyses. The analysis value was obtained as 78.68 kN. Fig. 15 shows the *P-Δ* curve of the two-bay combined system obtained from the numerical analysis.

5.2 Outdoor test and analysis on full-scale combined system of scaffolds and shores

5.2.1 Critical load of the overall structural system

In the test on the full-scale combined system of scaffolds and shores, sandbags were lifted and placed on predetermined positions on the slab one by one. When the 16th sandbag was placed on the slab, the whole combined system of scaffolds and shores collapsed suddenly without any warning.

Since the whole system collapsed while the 16th sandbag was being placed onto the slab, only half the weight of the 16th sandbag (2.373 kN) was counted. Table 2 shows the loading result from the sandbags. After considering the initial weight (2.5 kN) of the slab, including the formwork, cross bar, and plywood, the critical load of the overall combined system of scaffolds and shores was 77.512 kN, as shown in Table 2.

5.2.2 Relationship between load and displacement

A. In-plane direction

In the test, the largest lateral displacement occurred in the in-plane direction of the scaffold system. Based on the measurements of the theodolite in the in-plane direction of

(A) One-bay

(B) Two-bay

Fig. 13 Failure shapes of one-bay and two-bay combined system of scaffolds and shores in tests

Table 2 Loads and displacements measured in outdoor loading test of the combined system

Load no.	Weight of sandbag on crane scale	Cumulative weight of sandbags	In-plane (Theodolite I)			Out-of-plane (Theodolite II)		
			A_H	B_H	B_V	C_H	D_H	D_V
	kN	kN	mm	mm	mm	mm	mm	mm
1	4.737	7.237	1	0	0	1	0	0
2	4.894	12.131	1	0	0	1	0	0
3	4.795	16.926	2	1	0	4	0	0
4	4.835	21.761	3	1	0.5	5	0	0
5	4.844	26.605	3	1	0.5	5	0	0
6	4.746	31.352	9	2.5	3	7	0	0
7	4.835	36.187	10	2.5	3	7	0	1
8	4.805	40.992	12	2.5	3	7	0	1
9	4.864	45.856	13	2	3	7	0	1
10	4.903	50.759	18	1	2	7	0	2
11	4.874	55.633	19	2	3	7	0	2
12	4.903	60.536	24	2	4	8	0	2
13	4.844	65.381	28	2	4	8	0	3
14	4.835	70.216	35	2	5	8	0	3
15	4.923	75.139	41	3	5	7	0	3
16	2.373	77.512	46	4	5	8	0	3

Notes:
1. 11 3m long 6×6 stringers = 0.892 kN. 2. 4 4m long 6×9 stringers = 0.647 kN
3. 7 15mm thick 6'×9' clamps = 0.961 kN 4. Initial weight 0.892+0.647+0.961 = 2.5 kN
5. Since the whole system collapsed while the 16th sandbag was being placed on the slab, only half the weight of the 16th sandbag was counted
   (4.746/2=2.373 kN).

the scaffold system, as shown in Table 2, the load-displacement curves of "the joints between the bottom-end of the wooden shores and the top-end of the steel scaffolds" and "the joints between the top-end of the wooden shores and the top formwork" can be drawn as shown in Fig. 16.

Fig. 16 shows that, in the in-plane direction of the scaffold system, the lateral displacement of the top formwork is smaller than that at the joint between the bottom-end of the wooden shores and the top-end of the steel scaffold.
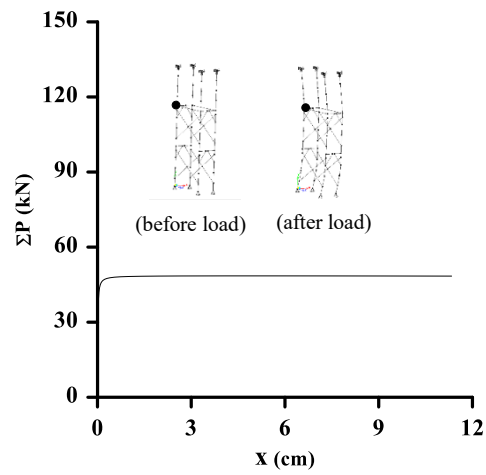
Fig. 14 *P-Δ* curve from numerical analysis of one-bay, two-story combined system of scaffolds and shores
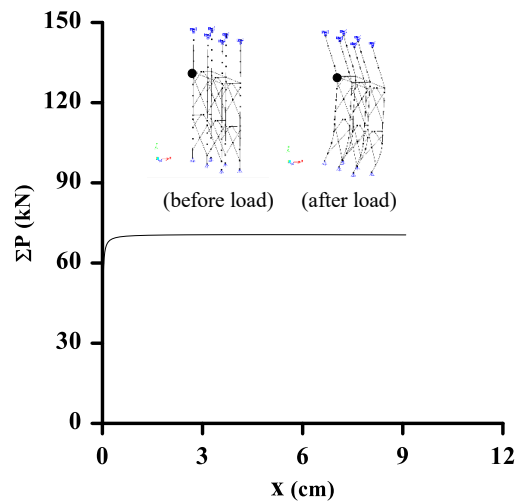

Fig. 15 *P-Δ* curve from numerical analysis of the two-bay, two-story combined system of scaffolds and shores
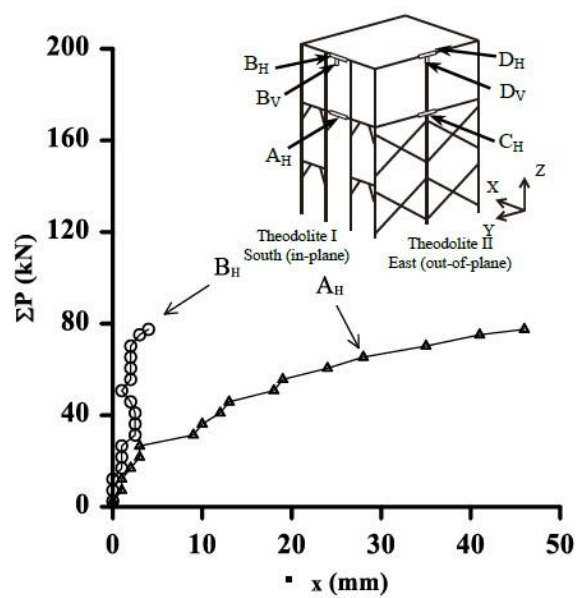

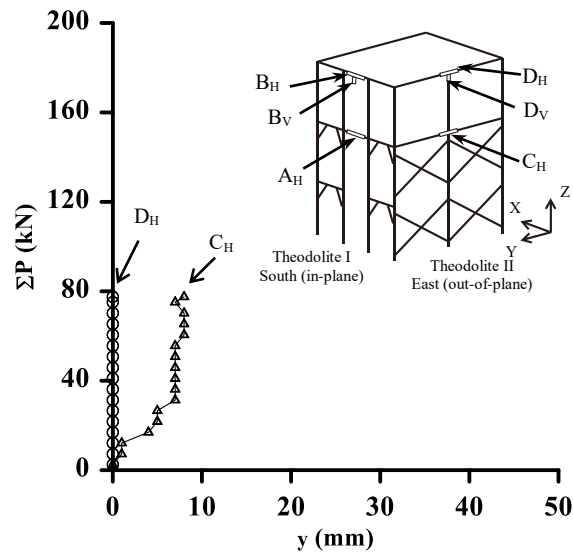Fig. 16 Lateral displacements vs. sandbag loads in the in-plane direction of combined system

Fig. 17 Lateral displacements vs. sandbag loads in the out-of-plane direction of combined system
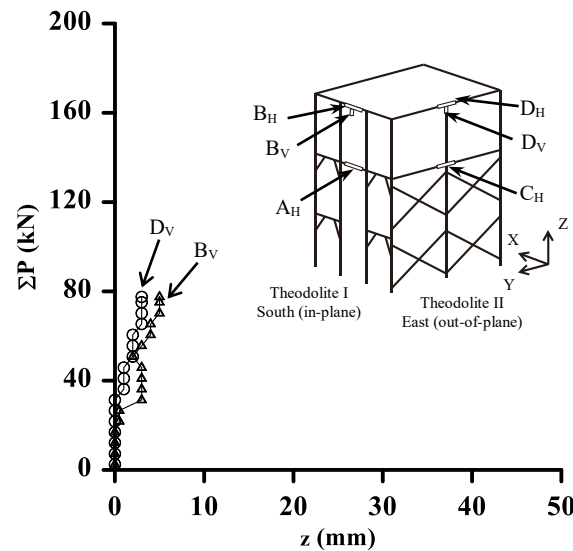

Fig. 18 Vertical displacements of the top formwork vs. sandbag loads for combined system

B. Out-of-plane direction

Based on the measured results by the theodolites in the out-of-plane direction of the scaffold system, as shown in Table 2, the load-displacement curves of "the joints between the bottom-end of the wooden shores and the top-end of the steel scaffolds" and "the joints between the top-end of the wooden shores and the top formwork" can be drawn in Fig. 17. As shown in Fig. 17, the displacements of the above-mentioned joints are not obvious, indicating that the deformation of the combined system of scaffolds and shores is not primarily in the out-of-plane direction of the combined system.

C. Vertical direction

Table 2 shows the vertical displacements measured by the theodolites at the joints between the top-end of the wooden shores and the top formwork. Fig. 18 shows the load-vertical displacement curves at the top formwork after loading. By comparison, the vertical displacements of the scaffold system are far smaller than its lateral displacements.

As shown in Fig. 18, the vertical displacements of the top formwork in the in-plane and out-of-plane directions of the scaffold system are close, indicating that in the loading process, the overall top formwork is evenly and vertically moving downward.

5.2.3 Axial force of scaffold steel tubes

Fig. 19 shows the relationship between the axial forces of various vertical scaffold steel tubes and loaded sandbag weights. In this scaffold installation, the central steel tubes (Nos. B_2 and B_3) bear the largest load while the outside steel tubes bear comparatively less load.

Fig. 20 shows the relationship between the lateral forces constraining the top formwork in the horizontal direction
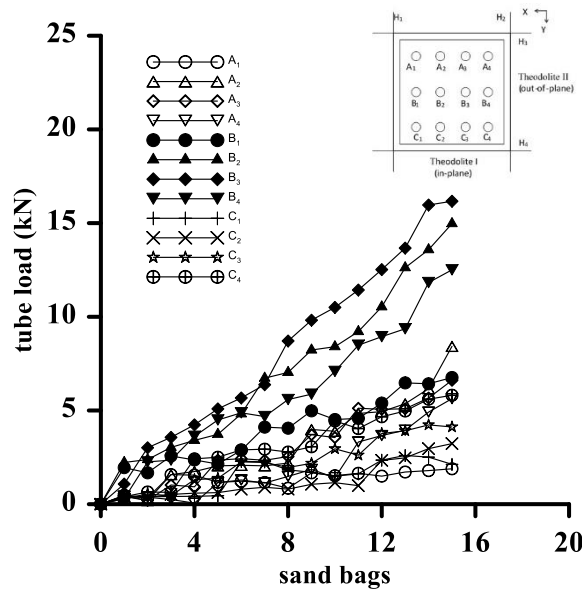
Fig. 19 Sandbag loads vs. axial forces of the vertical steel tubes in outdoor loading test of combined system
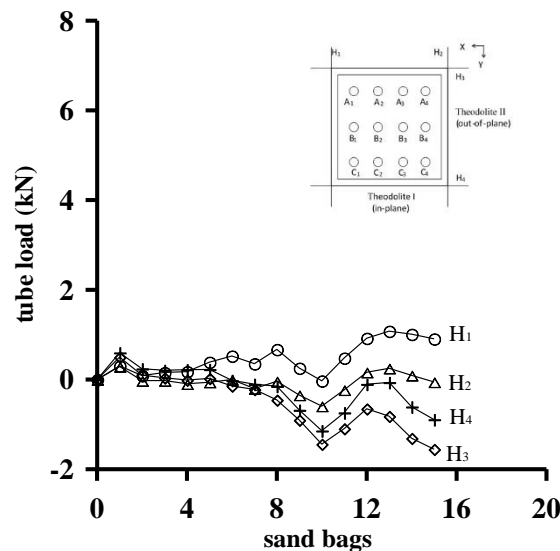

Fig. 20 Sandbag loads vs. lateral bracing force constraining the top formwork in outdoor loading test of combined system

and the loaded weights of the sandbags. The lateral forces constraining the top formwork are not obvious and do not change significantly, indicating that moderate lateral forces will be enough to constrain the top formwork of the combined system of scaffolds and shores from moving horizontally.

Fig. 21 shows the relationship between the cumulatively total vertical loads measured by the strain gauges and the cumulative weights of the sandbags in the outdoor loading test. The cumulative total vertical loads measured by the strain gauge is close to the cumulative weight of the sandbags in the loading test, indicating that the axial forces of the steel tubes measured by strain gauges are relatively reliable, as shown in Fig. 21.

5.2.4 Collapse of the combined system of scaffolds and shores

Fig. 22 shows the instant at which the collapse of the combined system of scaffolds and shores occurred, recorded in the in-plane direction of the combined system in the outdoor loading test. Similarly, Fig. 23 shows the moment of collapse of the combined system recorded in the out-of-plane direction in the outdoor loading test.

As shown in Steps 2 and 3 in Figs. 22 and 24, at the moment of collapse of the combined system, the failure did not occur on the scaffold or on the wooden shore. This indicates that the failure model of the combined system of scaffolds and shores in the outdoor loading test was buckling of the overall combined system rather than the failure caused by buckling of the scaffold or the wooden shore.
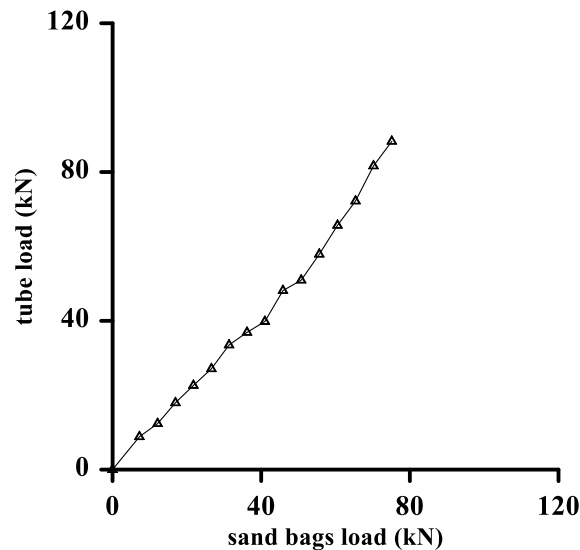
Fig. 21 Relationship between the cumulative loads measured by total strain gauge loads and sandbag weights in outdoor loading test of combined system

As shown in Steps 2 and 3 in Fig. 23, the failure of the combined system primarily occurred in the in-plane direction of the combined system because almost no displacement occurred in the out-of-plane direction.

5.2.5 Numerical analysis

In the numerical analysis for the combined system of scaffolds and shores, a second-order elastic analysis with semi-rigid joints was used. The parameters in the analysis are defined as follows: the bending stiffness of the tube joints in the scaffold was assumed as 2943 kN-cm/rad, the joint stiffness between the wooden shore and the scaffold is 981 kN-cm/rad, and the bottom of the scaffold were considered as hinged ends.

As shown in Fig. 16, during the loading process, minor lateral displacement of the top formwork was observed, indicating that the external steel frame could not provide a perfectly lateral support in test. In order to simulate this lateral displacement of the top formwork, two linear springs, with a stiffness of 0.05 kN/cm, were set up in the *X*- and *Y*-directions of the horizontal top formwork, respectively. The load distribution adopted in the analysis is shown in Fig. 25. This load distribution is based on the actual arrangement of sandbag loading in the outdoor loading test.

Based on the above assumptions for the stiffnesses of various joints in the combined system and the load distribution, the critical load of the combined system of scaffolds and shores is 74.6 kN based on the second-order elastic analysis with semi-rigid joints. The ratio of the test value (77.54 kN) to the analysis value (74.6 kN) is 1.04 (=77.54/74.6), indicating that they are extremely close.

Fig. 26 shows the comparison between the second-order analysis results and the test results of the combined system of scaffolds and shores. Through the comparison of load-displacement curves between the test and analysis values in Fig. 26, it was found that the on-site setup of the combined system in the outdoor test had a larger initial imperfection.

Suppose that the floor without lateral movements during grouting is restrained by the already dried reinforced concrete walls and columns. Based on this assumption, the slight lateral displacement of the top formwork in the outdoor test can be ignored in the actual analysis for on-site scaffolds. Thus, the boundary condition of the top formwork can be simulated as hinged ends without lateral horizontal displacement. In another second-order analysis with the same steps, the critical load of the combined system is obtained as 90.06 kN. The ratio of the test value (77.512 kN) to the analysis value (90.06 kN) is 0.86 (=77.54/90.06).

The above assumptions for different joint stiffnesses and hinged boundary conditions of the top formwork can be adopted in a second-order analysis for future structural strength analysis and design of the combined system of scaffolds and shores. If the top formwork is considered to have a lateral displacement due to a lack of lateral support reinforcement during grouting, the critical load obtained from the top formwork with the hinged restraint can be multiplied by a strength reduction factor ϕ. The strength reduction factor ϕ of the lack of reinforcement at the top formwork was 0.86 based on this outdoor test.

5.3 Preliminary design guidelines of combined systems based on analysis and test results

Based on the comparison and validation of the results of various loading tests and second-order elastic analyses with semi-rigid joints, this study proposes the preliminary design guidelines for engineers to design the strength of combined system of scaffolds and shores in the future. The key steps for implementation are described as follows:

(1). Install a one-bay, two-story scaffold system with different setups of bottom screw jacks and U-shaped top screw jacks in the structural testing laboratory. Conduct at least two tests on the scaffold system and then obtain the mean value of its load bearing capacity.

Step 1

Step 2
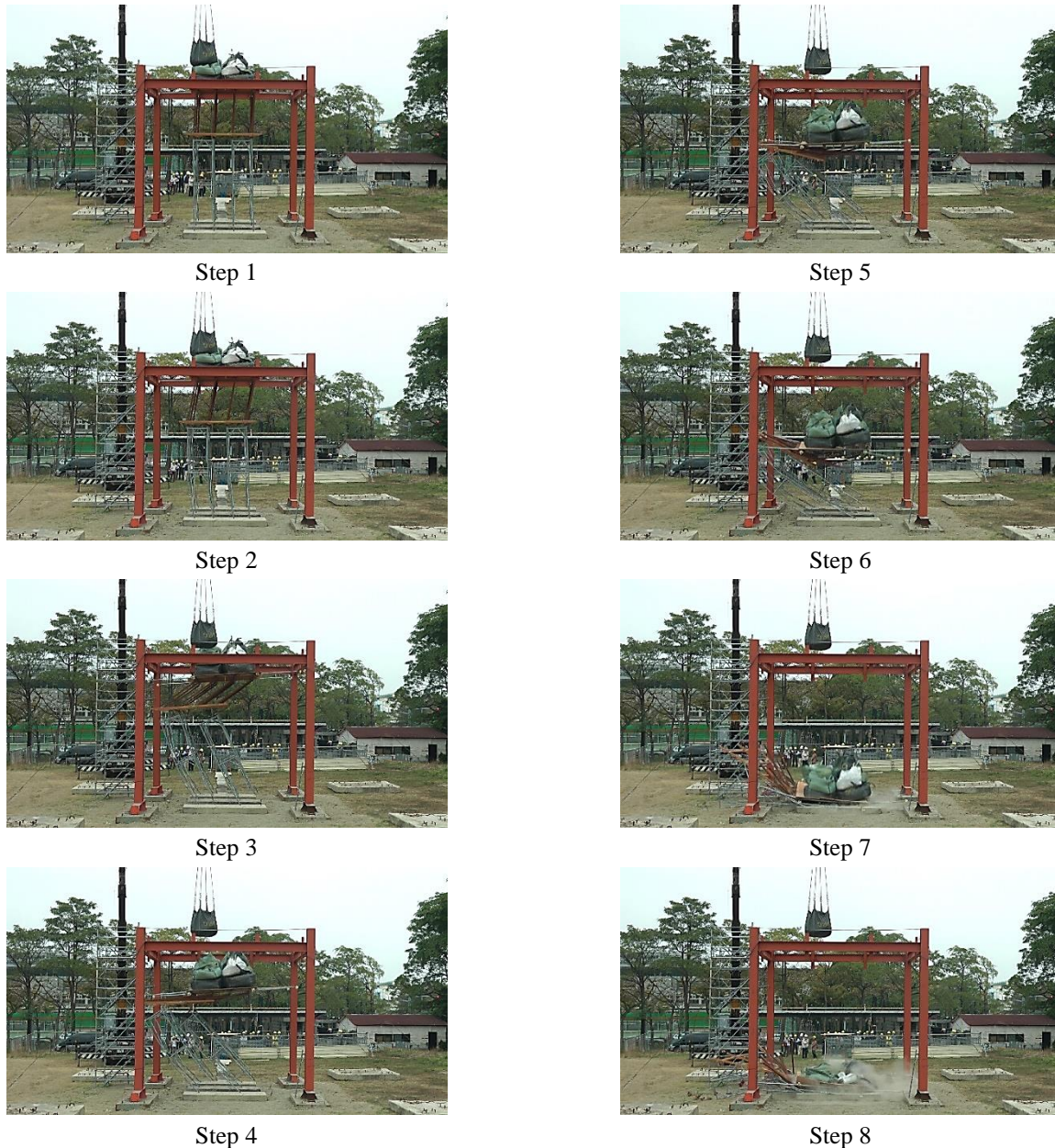
Step 3

Step 4

Step 5

Step 6

Step 7

Step 8

Fig. 22 Collapse moment in the in-plane direction of the combined system in outdoor loading test

(2). Conduct a second-order elastic analysis with semi-rigid joints for the setup of the above scaffold system, and then compare the analysis results with the various test results above in order to determine the bending stiffness values of the steel tube joints, bottom screw jacks, and U-shaped top screw jacks in the scaffold system.

(3). Install a one-bay combined system with two-story scaffolds and 1.7 m long shores in the structural testing laboratory. Conduct at least two tests on the combined system of scaffolds and shores, and then obtain the mean value of its load bearing capacity.

(4). Conduct the second-order elastic analysis with semi-rigid joints for the setup of the above combined system, and then compare the analysis results with the above test results in order to determine the bending stiffness value of the joint between the scaffold and top shores.

(5). Conduct the second-order elastic analysis with semi-rigid joints for the setup of the multi-bay, multi-row, multi-story combined system of scaffolds and shores based on the stiffness values of the various joints obtained above. This will allow the critical load and failure model of the combined system to be determined.

(6). Conduct the loading test of the full-scale combined system of scaffolds and shores. The setup is described in Step (5). If the structural testing laboratory is not big enough for the test setup of the full-scale combined system, the loading test of the full-scale combined system should be conducted outdoors. The results of the loading test can be used to verify the correctness of the load bearing capacity and failure model obtained from the second-order elastic analysis with semi-rigid joints in Step (5).
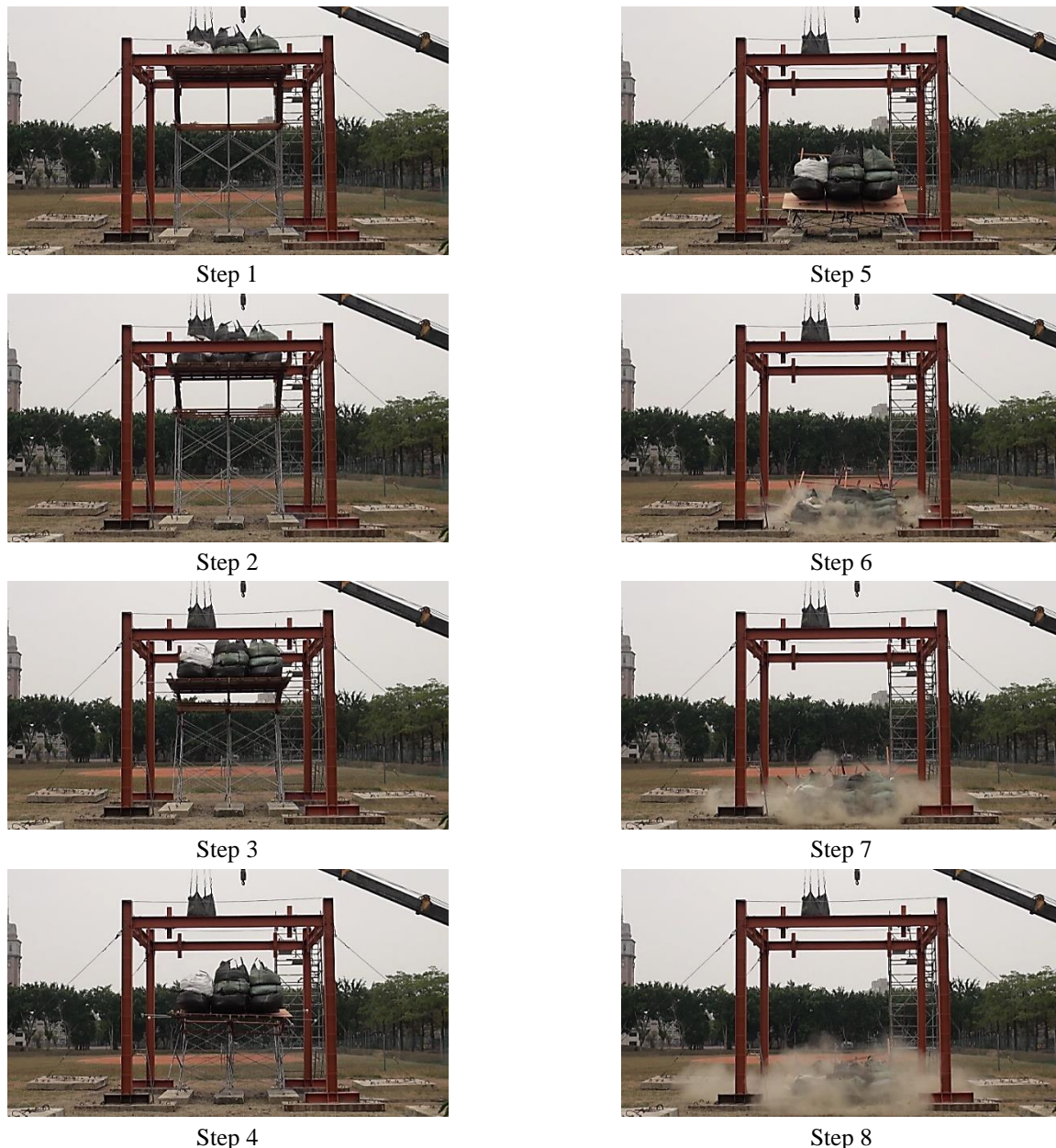
Fig. 23 Collapse moment in the out-of-plane direction of the combined system in outdoor loading test

(7). Through the comparison and validation between the analysis results in Step (5) and the test results in Step (6), the correctness of the bending stiffness values of various joints in the second-order elastic analysis with semi-rigid joints is confirmed. The structural strength design of the actual combined system of scaffolds and shores on construction sites can now be started.

6. Conclusions

This study investigates the structural stability and safety of the combined system of scaffolds and shores commonly used on construction sites in Taiwan. Apart from material tests, loading tests and a second-order elastic analysis with semi-rigid joints were also conducted in the study. Based on

the comparison of the test and analysis results, the bending stiffness values of various joints of the combined system were confirmed. The load bearing capacities and failure models of various scaffold systems were determined. Highlights of the results obtained in the study are as follows:

1. As shown by the results of the loading tests conducted in the structural testing laboratory, the load bearing capacity of the one-bay, two-story combined system of scaffolds and shores is about half that of the three-story scaffold system with the same height. The failure of the scaffold system begins with buckling of the steel tubes. When the deformation reaches the extent of yielding, the system fails. On the other hand, the failure of the combined system is due to buckling of the entire structural system. The failure models of these two structural systems are significantly different.

Fig. 24 No damage to components at collapse moment in combined system of scaffolds and shores in outdoor loading test
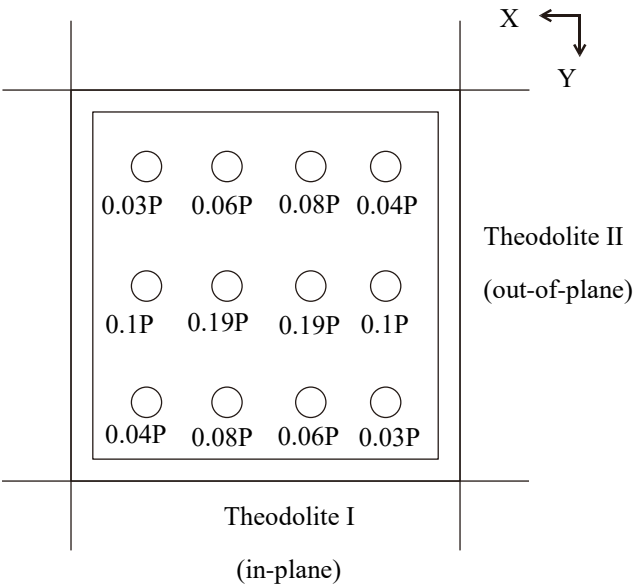

Fig. 25 Load distribution on top formwork of the combined system in the second-order analysis

2. As shown by the results of the outdoor loading test on the combined system of scaffolds and shores, when the combined system fails, the scaffolds and wooden shores are intact without obvious signs of buckling, yielding, or breaking. In other words, when the combined system collapses, all members in the system are intact. The failure of the combined system is due to "systematic buckling" of the entire structure. It is not advisable to adopt the combined system of scaffolds and shores on construction sites. It is advised to use scaffold with only one type of steel scaffold in order to reduce the risk of collapse.

3. Based on the comparison between the analysis and test results in different setups of scaffold systems, it was confirmed that the second-order elastic analysis with semi-rigid joints is suitable for determining the load bearing capacities and failure models of various scaffold systems. After summarizing the determination processes of various joint stiffnesses in scaffold systems, this study proposed the preliminary structural design guidelines for the combined system of scaffolds and shores, which may serve as the reference for engineers in designing for the structural strength of future combined system of scaffolds and shores.
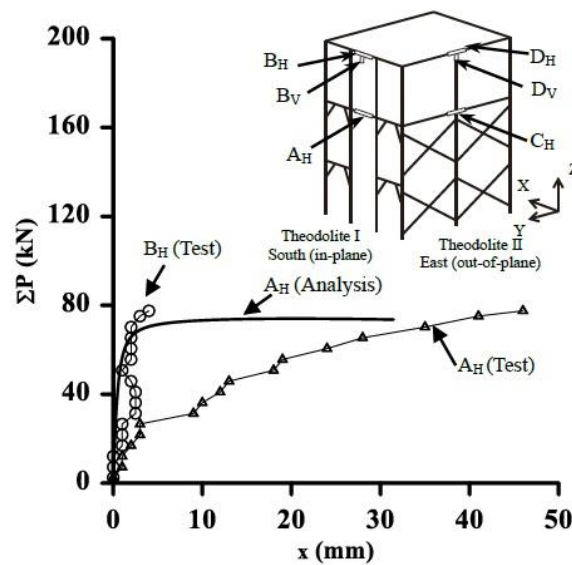
Fig. 26 P-Δ curves in the in-plane direction of the combined system based on outdoor loading test and second-order analysis

4. The load bearing capacity of the combined system of scaffolds and shores increases with increasing bay numbers, however not in integral multiples. The deformations of both "the scaffold system" and "the combined system of scaffolds and shores" after being loaded mainly occur in the in-plane direction of the scaffold systems.

5. In the outdoor loading test of the combined system of scaffolds and shores, after the sandbags were loaded, the change of axial force of the steel tubes in the scaffolds was consistent with the positions and sequences of the sandbags being loaded. The central steel tubes bear larger loads than the outside ones. In addition, the lateral support force and displacement of the top formwork were minor, indicating that the top formwork of the combined system can achieve the effect of lateral support reinforcement without much lateral support force.

6. In order to enhance the load bearing capacity of the combined system of scaffolds and shores, it is advisable to set up horizontal lateral supports at the joints between the scaffolds and wooden shores in the in-plane direction of the scaffold as the reinforcement to reduce the displacement at these joints and then enhance the load bearing capacity of the whole structural system.

Acknowledgements

References

Błazik-Borowa, E. and Gontarz, J. (2016), "The Influence of the Dimension and Configuration of Geometric Imperfections on the Static Strength of a Typical Façade Scaffolding", *Archiv. Civil Mech, Eng.*, **16**(3), 269-281. https://doi.org/10.1016/j.acme.2015.11.003.

Chandrangsu, T. and Rasmussen, K.J.R. (2011), "Structural Modelling of Support Scaffold Systems", *J. Constr. Steel Res.*, **67**(5), 866–875. http://dx.doi.org/10.1016/j.jcsr.2010.12.007.

Chan, Jake L.Y. and Lo, S.H. (2019), "Direct analysis of steel frames with asymmetrical semi-rigid joints", *Steel Compos. Struct.*, **31**(1), 99-112. https://doi.org/10.12989/scs.2019.31.1.099.

Chan, S.L. and Zhou, Z.H. A., (1994), "Pointwise equilibrium polynomial (pep) element for nonlinear analysis of frame", *J. Struct. Eng. - ASCE*, **120**(6), 1703-1717. https://doi.org/10.1061/(ASCE)0733-9445(1994)120:6(1703).

Chan, S.L., Zhou, Z.H., Chen, W.F., Peng, J.L. and Pan, A.D., (1995), "Stability Analysis of Semi-rigid Steel Scaffolding", *Eng. Struct.*, **17**(8), 568-574. https://doi.org/10.1016/0141-0296(95)00011-U.

Cimellaro, G.P. and Domaneschi, M. (2017), "Stability Analysis of Different Types of Steel Scaffolds", *Eng. Struct.*, **152**(1), 535-548. http://dx.doi.org/10.1016/j.engstruct.2017.07.091.

Gohnert, M., Li, K. and Son, K.S. (2016), "Experimental Investigation on the Load Capacity of a Scaffolding Frame", *Int. J. Eng. Tech.*, **8**(6), 2460-2467. DOI:10.21817/ijet/2016/v8i6/160806198

Ilcik, J., Arora, V. and Dolejs, J. (2016), "Design of new scaffold anchor based on the updated finite element model", *Eng. Struct.*, **118**(1), 334-343. http://dx.doi.org/10.1016/j.engstruct.2016.03.064.

Jia, L., Liu, H., Chen, Z., Liu, Q. and Wen, S. (2016), "Mechanical Properties of Right-Angle Couplers in Steel Tube-Coupler

Scaffolds", *J. Constr. Steel Res.*, **125**, 43-60. http://dx.doi.org/10.1016/j.jcsr.2016.06.005.

Kuo, C.C., Peng, J.L., Yen, T. and Chan, S.L (2008), "Experimental Study of Modular Falsework System with Wooden Shores under Various Path Loads", *Adv. Struct. Eng.*, **11**(4), 369-382. http://dx.doi.org/10.1260/136943308785836844.

Liu, H., Chen, Z., Wang, X. and Zhou, T. (2010a), "Theoretical analysis and experimental research on stability behavior of structural steel tube and coupler falsework with X-bracing", *Adv. Steel Constr.*, **6**(4), 949-962. DOI:10.18057/IJASC.2010.6.4.2

Liu, H. Jia, L., Wen, S., Liu, Q., Wang, G. and Chen, Z. (2016), "Experimental and Theoretical Studies on The Stability of Steel Tube-Coupler Scaffolds with Different Connection Joints", *Eng. Struct.*, **106**(1), 80-95. http://dx.doi.org/10.1016/j.engstruct.2015.10.015.

Liu, H., Zhao, Q., Wang, X., Zhou, T., Wang, D., Liu, J. and Chen, Z. (2010b), "Experimental and analytical studies on the stability of structural steel tube and coupler scaffolds without X-bracing", *Eng. Struct.*, **32**(4), 1003-1015. http://dx.doi.org/10.1016/j.engstruct.2009.12.027.

Liu, S.W., Chan, Jake L.Y., Bai, R. and Chan, S.L., (2018), "Curved-quartic-function elements with end-springs in series for direct analysis of steel frames", *Steel Compos. Struct.*, **29**(5), 623-633. https://doi.org/10.12989/scs.2018.29.5.623.

Nguyen, P.C. and Kim, S.E. (2016), "Advanced analysis for planar steel frames with semi-rigid connections using plastic-zone method", *Steel Compos. Struct.*, **21**(5), 1121-1144. https://doi.org/10.12989/scs.2016.21.5.1121.

NIDA (2018), "User Manual and Analysis Theory", Version 10.0.

Peng, J.L., Ho, C.M., Lin, C.C. and Chen, W.F. (2015), "Load-Carrying Capacity of Single-Row Steel Scaffolds with Various Setups", *Adv. Steel Constr.*, **11**(2), 185-210. DOI:10.18057/IJASC.2015.11.2.4

Peng, J.L., Wang, C.S., Wu, C.W. and Chen, W.F. (2017), "Experiment and Stability Analysis on Heavy-Duty Scaffold Systems with Top Shores", *Adv. Steel Constr.*, **13**(3), 293-317. DOI: 10.18057/IJASC.2017.13.3.6

Pieńko, M. and Błazik-Borowa, E. (2013), "Numerical Analysis of Load-bearing Capacity of Modular Scaffolding Nodes", *Eng. Struct.*, **48**, 1-9. https://doi.org/10.1016/j.engstruct.2012.08.028.

Prabhakaran, U., Beale, R.G. and Godley, M.H.R. (2011), "Analysis of scaffolds with connections containing looseness", *Comput. Struct.*, **89**, 1944-1955. http://dx.doi.org/10.1016/j.compstruc.2011.03.016.

Sevim, B., Bekiroglu, S. and Arslan, G. (2017), "Experimental Evaluation of Tie Bar Effects on Structural Behavior of Suspended Scaffolding Systems", *Adv. Steel Constr.*, **13**(1), 62-77. DOI: 10.18057/IJASC.2017.13.1.4

Thai, H.T., Kim, S.E. and Kim, J. (2017), "Improved refined plastic hinge analysis accounting for local buckling and lateral-torsional buckling", *Steel Compos. Struct.*, **24**(3), 339- 349. https://doi.org/10.12989/scs.2017.24.3.339.

Yue, F., Yuan, Y., Li, G.Q., Ye, K.M., Chen, Z. and Wang, Z. (2005), "Wind Load on Integral-Lift Scaffolds for Tall Building Construction", *J. Struct. Eng. - ASCE*, **131**(5), 816-824. http://dx.doi.org/10.1061/(ASCE)0733-9445(2005)131:5(816).

Zhang, H., Chandrangsu, T. and Rasmussen, K.J.R. (2010), "Probabilistic Study of The Strength of Steel Scaffold Systems", *Struct. Saf.*, **32**(6), 393-401. http://dx.doi.org/10.1016/j.strusafe.2010.02.005.

Zhang, H., Rasmussen, K.J.R. and Ellingwood, B.R. (2012), "Reliability assessment of steel scaffold shoring structures for concrete formwork", *Eng. Struct.*, **36**, 81-89. http://dx.doi.org/10.1016/j.engstruct.2011.11.027.

Zhao, Z. and Chen, Z. (2016), "Analysis of door-type modular steel scaffolds based on a novel numerical method", *Adv. Steel Constr.*, **12**(3), 316-327. DOI: 10.18057/IJASC.2016.12.3.6

DL